Mapping Substrate-Induced Conformational Changes in cAMP-Dependent Protein Kinase by Protein Footprinting†

Xiaodong Cheng,‡ Shmuel Shaltiel,§ and Susan S. Taylor*,‡

Howard Hughes Medical Institute and Department of Chemistry and Biochemistry, University of California, San Diego, La Jolla, California 92093-0654, and Department of Biological Regulation, The Weizmann Institute of Science, Rehovot 76100, Israel

Received May 7, 1998; Revised Manuscript Received July 22, 1998

ABSTRACT: Upon binding of substrates the catalytic subunit (C) of cAMP-dependent protein kinase (cAPK) undergoes significant induced conformational changes that lead to catalysis. For the free apoenzyme equilibrium favors a more open and malleable conformation while the ternary complex of C, MgATP, and a 20-residue inhibitor peptide [PKI (5−24)] adopts a tight and closed conformation [Zheng, J., et al. (1993) *Protein Sci. 2*, 1559]. It is not clear that binding of either ligand alone is responsible for this conformational switch or whether both are required. In addition, the catalytic subunit binds MgATP and inhibitor peptide synergistically. The structural basis for this synergism is also not defined at present. Using an Fe−EDTA-mediated protein footprinting technique, the conformational changes associated with the binding of MgATP and the heat stable protein kinase inhibitor (PKI) were probed by mapping the solvent-accessible surface and structural dynamics of C. The conformation of the free enzyme was clearly distinguished from the ternary complex. Furthermore, binding of MgATP alone induced extensive conformational changes, both local and global, that include the glycine-rich loop, the linker connecting the small and large lobes, the catalytic loop, the Mg^{2+} positioning loop, the activation loop, and the F helix. These changes, similar to those seen in the ternary complex, are consistent with a transition from an open to a more closed conformation and likely reflect the motions that are associated with catalysis and product release. In contrast, the footprinting pattern of C·PKI resembled free C, indicating minimal conformational changes. Binding of MgATP, by shifting the equilibrium to a more closed conformation, "primes" the enzyme so that it is poised for the docking of PKI and provides an explanation for synergism between MgATP and PKI.

Protein phosphorylation is one of the most important processes for cellular regulation and signal transduction in the eukaryotic cell. Despite their considerable diversity, eukaryotic protein kinases, which catalyze the phosphorylation reaction, have apparently evolved, in part, from a common origin and share a conserved catalytic core (*1*, *2*). cAMP-dependent protein kinase (cAPK)[1] is one of the best characterized and simplest members of this family (*3*, *4*). The crystal structure of the catalytic subunit (C) of cAPK was the first protein kinase structure to be solved (*5*) and has served subsequently as a prototype for the entire family (*6*, *7*). This structure reveals that the catalytic core adopts a bilobal fold with MgATP deeply buried in the active site cleft between the two lobes where catalysis occurs. Most of the invariant residues in the protein kinase core cluster around the active site cleft and contribute either to nucleotide binding or to phosphoryl transfer (*8*). At the mouth of the cleft, where peptide substrates bind, is the "activation loop", a major structural element involved in regulating kinase activity (*5*, *8*, *9*). Structures of several other protein kinases reveal that the activation loop is one of the most variable regions of the protein. The activation of protein kinases requires this loop to be properly oriented, and in many cases the activation event itself is controlled by phosphorylation of the activation loop on conserved Thr, Ser, or Tyr residues (*10*−*16*). In contrast to many protein kinases where phosphorylation of the activation loop is very dynamic, the C subunit is constitutively phosphorylated on Thr197 on the activation loop. This phosphate is very stable (*17*). The regulation of the catalytic subunit of cAPK is typically through interaction with an inhibitory regulatory (R) subunit which sequesters the C subunit in an inactive state under physiological conditions. Activation is then achieved by the generation of cAMP which binds to the R subunit, thereby reducing its affinity for the C subunit and leading to activation of the complex (*4*, *6*).

Catalysis by C requires binding of both MgATP and a protein or peptide substrate. Several crystal structures of the active C subunit complexed with various ligands have been solved, and these structures reveal open, closed, and intermediate conformations. Conformational flexibility is

† This work was supported by NIH Grant GM19301 to S.S.T. and by grants from the Minerva Foundation and the German−Israeli Foundation for Scientific Research and Development to S.S. X.C. was supported by American Cancer Society Postdoctoral Fellowship PF-4315.

‡ University of California, San Diego.

§ The Weizmann Institute of Science.

[1] Abbreviations: C, cAMP-dependent protein kinase catalytic subunit; cAPK, cAMP-dependent protein kinase; Caps, 3-(cyclohexylamino)-1-propanesulfonic acid; CNBr, cyanogen bromide; Mops, 3-(*N*-morpholino)propanesulfonic acid; NCS, *N*-chlorosuccinimide; PKI, heat stable protein kinase inhibitor; R, cAMP-dependent protein kinase regulatory subunit; Tris, tris(hydroxymethyl)aminomethane.

S0006-2960(98)01057-5 CCC: $15.00
Published on Web 09/17/1998

critical for catalysis. The transition state is thought to require a fully closed conformation with the backbone amide of Ser53 at the tip of the glycine-rich loop forming a hydrogen bond with the γ-phosphate of ATP. On the other hand, the release of ADP, the rate-limiting step in catalysis, requires the opening of the active site cleft (*18*, *19*). While crystal structures of the binary [C·PKI(5−24)] and ternary [C·PKI(5−24)·ATP] complexes of recombinant mouse C_α showed no major conformational differences with the exception of the glycine-rich loop (*8*, *20*), crystallographic studies of mammalian porcine C revealed a more open conformation for the free apoenzyme and binary complex and a closed conformation for the ternary complex (*21*−*23*). It is not clear at present which substrate is responsible for the conformational switch that is necessary for the catalysis. Clearly, in the presence of both MgATP and PKI equilibrium strongly favors the closed conformation whereas in the absence of ligands the structure adopts an open or malleable conformation.

A novel protein footprinting technique was used here to probe the changes in protein conformation and dynamics of the catalytic subunit associated with the binding of substrate and inhibitor, in particular to determine whether one substrate preferentially serves as a conformational switch. Protein footprinting, a technique analogous to DNA footprinting, has been described and applied recently to mapping contact domains and conformational changes of proteins involved in protein−DNA, protein−protein, and protein−ligand interactions (*24*−*31*). In this approach, the solvent-accessible surface of a specific protein is mapped by proteases or chemical cleavage reagents. By comparison of the cleavage pattern of the free and ligand-associated proteins, surface protection and conformational changes induced by ligand association can be probed. Use of end-labeled protein allows precise identification of sites of cleavage along the linear protein sequence, and the use of free radicals generated by an Fe−EDTA complex as a chemical cleavage reagent permit high-resolution probing of a protein surface. Most important, our study provided detailed information on global ligand-induced conformational changes in cAPK at the molecular level under equilibrium solution conditions.

EXPERIMENTAL PROCEDURES

Materials. Wild-type murine C_α was overexpressed in *Escherichia coli* BL21-DE3 using the pLWS-3 vector (*32*) and purified as described previously (*33*). Isozyme II phosphorylated on Ser10, Thr197, and Ser338 was pooled and used for all experiments. Protein concentration was determined using an absorption coefficient of 48 000 M^{-1} cm^{-1} at 280 nm. The heat stable protein kinase inhibitor, PKI (isoform α), was expressed and purified as described previously (*34*). All proteins were homogeneous as judged by SDS−polyacrylamide gel electrophoresis. Horseradish peroxidase conjugated anti-rabbit IgG (donkey) and ECL western blotting detection reagent kits were obtained from Amersham Life Science.

Preparation of N- and C-Terminal Antibodies of C. Antibodies that are specific to the N- and C-terminus of C were generated using synthetic peptides ^{6}AKKGSEQES-VKEFLAKAK^{23} and ^{338}SINEKCGKEFSEF^{350}, where the numbers correspond to the position of the amino acid residues in the C subunit sequence. These peptides were synthesized on a solid-phase synthesizer, purified by reverse-phase HPLC, and analyzed by amino acid composition and sequencing before use. Purified peptides were then cross-linked with KLH (Pierce) as a carrier, and the resulting conjugates were used for immunization. All the anti-peptide antibodies used in the present study were affinity purified as described below. The immune sera obtained were fractionated by an ammonium sulfate precipitation (repeated twice), and the resulting IgG fractions were passed through a column with immobilized KLH to remove the anti-KLH-specific antibodies and further purified on an affinity column of agarose beads with the corresponding peptide immobilized. The specificity of the antibodies was tested and confirmed by deletion mutants of C (*35*).

Fe−EDTA Chemical Cleavage Reaction. Cleavage reactions were performed in buffer containing 10 mM Mops, 50 mM NaCl, and 10 mM $MgCl_2$ (pH 7.2) at room temperature. A typical reaction (final volume of 50 μL) contained 16 μM purified C, 5 mM ATP, and 32 μM PKI when present in the reaction. The initial reaction mixture (35 μL) of enzyme, substrate, and inhibitor was incubated at room temperature for 30 min. The cleavage reaction was started by simultaneous addition of 5 μL each of freshly prepared 10× ($FeSO_4$, EDTA), ascorbate (pH adjusted to 7.2), and H_2O_2 to a final concentration of (1, 2), 20, and 1 mM, respectively. After incubation for an additional 20 min, the reaction was stopped by addition of 17 μL of 4× sample loading buffer (50 mM Tris, 4% SDS, 12% glycerol, 2% β-mercaptoethanol, 0.01 bromophenol blue, pH 6.8) and stored at −80 °C until being loaded onto the gel. Alternatively, 10 μL of ethanol, a free radical quencher, was added to the sample at the end of the reaction, and the sample was then frozen and dried under speed-vac. The sample was dissolved in 30 μL of 1× sample loading buffer before being loaded.

Identification of the Cleavage Fragments. The cleavage products were separated on a discontinuous Tricine−SDS−PAGE system according to Schägger and Jagow (*36*). Protein samples were incubated at 50 °C for 10 min and loaded onto a 16 cm long slab gel with 16.5% separating, 10% spacing, and 4% stacking gels. All electrophoresis runs started at 30 V constant until protein samples completely entered the gel, and then the voltage was raised to 90−120 V. The run was stopped when the tracking dye ran out of the gel. After electrophoresis, proteins were transblotted onto a PVDF (0.1 μm, Millipore, or 0.2 μm, Bio-Rad) membrane. The electroblotting was performed in 10 mM Caps and 10% methanol (pH 11) buffer at 200 mA constant current for 1 h. The membrane was blocked with 5% nonfat milk in TTBS buffer (50 mM Tris, 150 mM NaCl, 0.1% Tween, pH 7.5) for 1−16 h. The membrane was probed with purified anti C- or N-terminal antibodies (1:10 000) in TTBS buffer containing 5% nonfat milk for 1 h. After three 10 min washes with TTBS buffer, the membrane was further blotted with HRP-conjugated secondary antibody (1:2 500) in TTBS buffer containing 5% nonfat milk for 45 min to 2 h. The membrane was then extensively washed with TTBS buffer (15 min for 4 times) and incubated with ECL reagents for 1−2 min. Detection of protein bands was achieved by exposing a sheet of autoradiography film (Kodak Hyperfilm-ECL) using the membrane with various exposure times. Once the proper image was obtained, the ECL film was further

digitalized and analyzed by Alphaimager 2000 to determine the electrophoretic mobility of the cleavage fragments.

Intrinsic Molecular Markers and Assignment of Cleavage Sites. Accurate assignment of the Fe−EDTA cleavage sites relies on the correct estimation of the molecular size of the cleavage fragments, which in turn depends on the correlation between the protein samples and standard molecular markers. Since correlation between molecular size and electrophoretic mobility varies from protein to protein, use of commercial molecular weight standards may not provide the accuracy needed for high-resolution mapping of the conformational changes in C for this study. To circumvent this problem, a set of intrinsic molecular markers was generated by partial specific cleavage of the catalytic subunit at Met and Trp residues (*37*). Briefly, the catalytic subunit was extensively dialyzed against 100 mM NH_4HCO_3 and lyophilized to remove salt before use. Site-specific partial cleavage at methionine residues was achieved by dissolving 100 μg of C in 50 μL of 4 mg/mL CNBr in 70% formic acid. After incubation at room temperature for 30 min, the cleavage reaction was terminated by addition 1 mL of water followed by freeze-drying. For site-specific partial cleavage at tryptophan residues, 100 μg of C was dissolved in 5.65 μL of 88% formic acid, followed by 40 μL of glacial acetic acid and 4.35 μL of water. The cleavage reaction was initiated by addition of 50 μL of 2 mg/mL NCS in 80% acetic acid. The reaction was incubated at room temperature for 15−60 min and stopped by addition of 1 mL of 3 mM methionine and freeze-drying. Dried peptides was dissolved in 50 μL of gel sample buffer right before loading.

To assign the positions of Fe−EDTA cleavage sites, we ran the Fe−EDTA cleaved sample along with the partially cleaved peptide fragments (2−5 μL) as molecular weight markers. The measured relative mobilities of these defined C fragments were plotted against their molecular weights (calculated by Peptide Tools). The standard curve was obtained by connecting the neighboring data points on the plot. The molecular weights of the Fe−EDTA cleavage fragments were calculated on the basis of their electrophoretic mobilities using the standard curve. The sites of the cleavage were derived using Peptide Tools (Hewlett-Packard) based on their calculated molecular weights.

Estimation of the Extent of Protein Damage during Fe−EDTA Cleavage. The percentage of the uncleaved catalytic subunit molecules remaining after exposure to Fe−EDTA was determined by comparing the intensity of the intact protein bands on SDS−PAGE before and after Fe−EDTA treatment. The enzymatic activity of the catalytic subunit, withdrawn at various times during the footprinting reaction, was measured and compared to that of the untreated sample to estimate the extent of overall damage of the catalytic subunit under reaction conditions.

RESULTS

Conditions for the Fe−EDTA Cleavage Reaction. Several conditions need to be satisfied for the Fe−EDTA cleavage reaction to be useful for protein footprinting studies: (1) the cleavage reagent itself should not perturb the protein under study prior to cleavage; (2) the cleavage of the protein molecule should be rather nonspecific so that the entire protein surface can be evenly sampled; (3) most importantly,

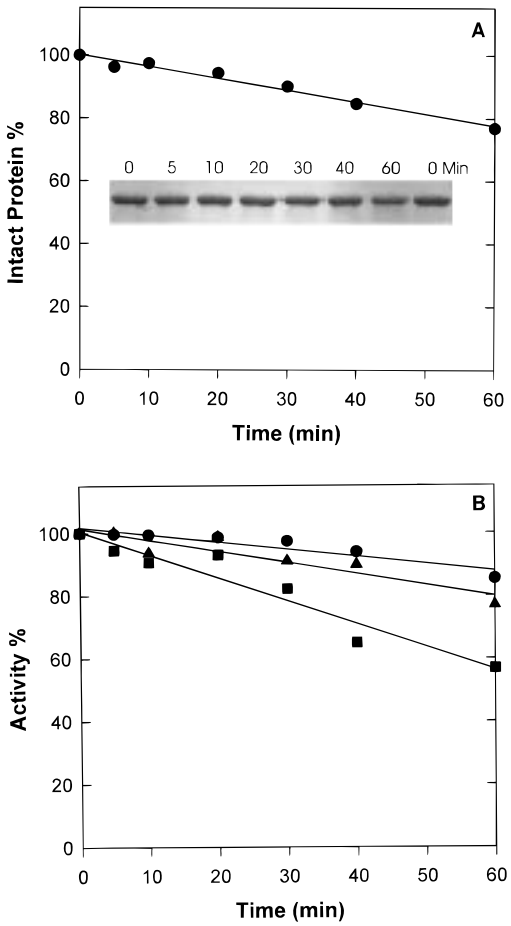

FIGURE 1: Extent of cleavage of the catalytic subunit by Fe−EDTA as a function of time. (A) Percentage of uncleaved catalytic subunit remaining as a function of cleavage time. The insert shows the original data of the SDS−PAGE gel. (B) Percentage of remaining enzymatic activity of the catalytic subunit as a function of time exposure to cleavage reagent. Curves: (●) C in the absence of cleavage reagent; (▲) and (■) C with and without 5 mM ATP, respectively. Experimental conditions were described in Materials and Methods.

conditions must be found whereby no more than one cleavage occurs in any molecular complex during the time course of the cleavage reaction. Maintaining "single cleavage" conditions is essential to ensure that we are probing the conformation of the native protein, not the secondary products of previous cleavage. Single cleavage conditions can be satisfied if the majority of the protein molecules remain uncut (*38*). Under the reaction conditions of this study, more than 90% of the protein remained uncut and more than 90% of the enzymatic activity was retained after 20 min of Fe−EDTA treatment (Figure 1). Our cleavage reaction conditions thus impose minimal structural and functional perturbations on the catalytic subunit, and the probability of multiple cleavage events occurring in any single catalytic subunit is negligible. In addition, even after 60 min of Fe−EDTA treatment, the only protein band detectable by Commassie staining was the uncut catalytic subunit; no other predominant cleavage products were visible (Figure 1A). This observation suggests that Fe−EDTA cleavage of C is fairly random and nonspecific.

Intrinsic Molecular Markers of Partially Cleaved C. To accurately assign Fe−EDTA cleavage sites, fragments generated by partial cleavage of the catalytic subunit at specific

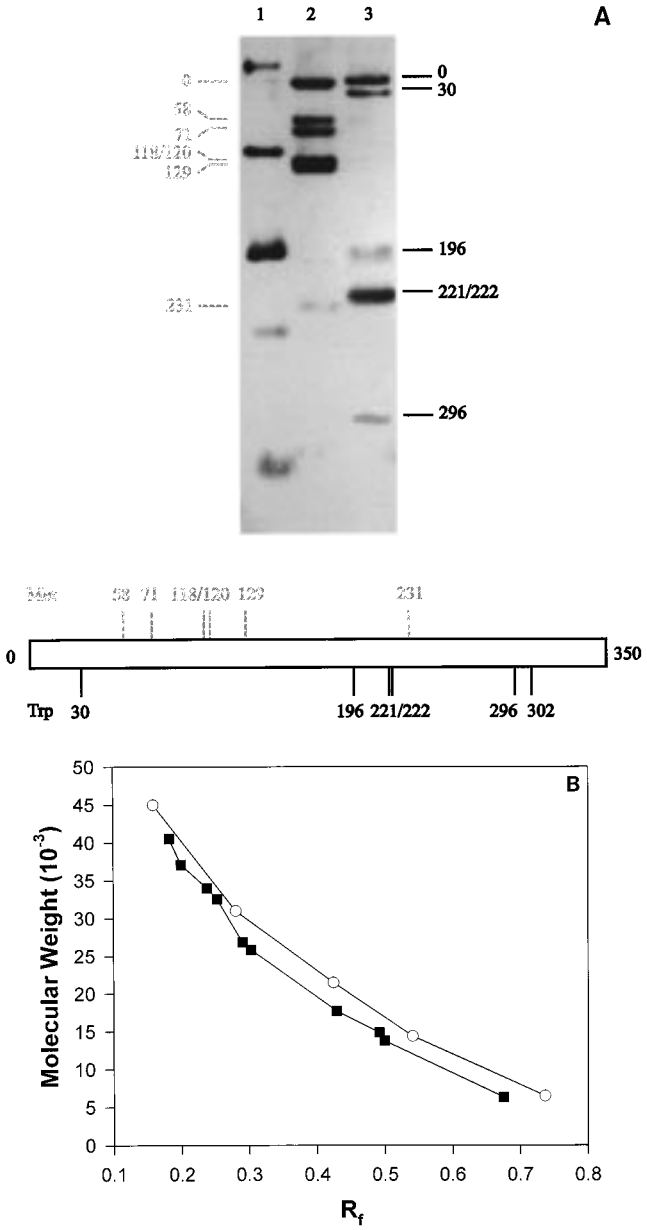

FIGURE 2: Intrinsic molecular weight markers of the catalytic subunit. (A) Lane 1: commercial biotinylated MW standards (Bio-Rad) with molecular weights of 45 000, 31 000, 21 500, 14 400, and 6500. Lanes 2 and 3: partially digested catalytic subunit fragments (visualized by anti C-terminal C antibodies) generated by methionine-specific cleavage at residues 58, 71, 118, 120, 129, and 231 (gray labels) and tryptophan-specific cleavage at positions 30, 196, 221, 222, 296, and 302 (black labels), respectively. (B) Molecular weight standard curves of intrinsic molecular markers (filled squares) and commercial molecular markers (open circles).

residues were used as a set of intrinsic molecular weight markers. The catalytic subunit contains six methionines and six tryptophans. Since these residues are distributed over about 80% of the catalytic subunit sequence from residues 30 to 302, they are ideal markers for position calibration. When probed by anti terminal C antibodies, partial cleavage at methionine residues by CNBr generated fragments terminating at residues 58, 71, 118/120, 129, and 231 while fragments terminating at positions 30, 196, 221/222, and 296 were obtained by Trp-specific cleavage with NCS (Figure 2A). The use of intrinsic molecular markers is necessary and critical for precise assignment of the cleavage sites since use of commercial standard molecular markers would lead to constant overestimation of the size of the cleavage product by 1000−4000 (Figure 2B).

Fe−EDTA Cleavage of the Catalytic Subunit and Assignment of Cleavage Sites. When the catalytic subunit was subjected to Fe−EDTA cleavage, many discrete polypeptide bands were identified by using a combination of anti N- and C-terminal C_α antibodies (Figure 3A,B). The localization of these sites confirmed that only solvent-exposed protein surfaces are susceptible to the Fe−EDTA cleavage. The use of anti terminal antibodies allows selective visualization of those cleavage products that start from the N-terminus or end at the C-terminus. Using residue-specific partial cleavage fragments as molecular weight standards, molecular weights of these terminal-containing cleavage products were determined. The locations of the cleavage sites that lead to the formation of these cleavage products were further deduced from their determined molecular weights. Large fragments detected by anti N-terminal antibodies were derived from cleavage sites close to the C-terminal end of the protein while large fragments probed by anti C-terminal antibodies resulted from cuts near the N-terminus. We were unable to locate cleavage sites close to the C-terminus using the anti C-terminal C_α antibodies and vice versa because the corresponding cleavage products were poorly retained on the PVDF membrane during the transfer. These short peptides were also less sensitive to immunodetection (Figure 3A). However, cleavage sites close to the C-terminus of the protein can be visualized using the anti N-terminal C antibodies (Figure 3B). A total of 35 unique cleavage sites were identified combining the use of anti N- and C-terminal C_α antibodies. These cleavage sites cover more than 85% of the catalytic subunit sequence spanning from residues 32 to 329 (Figure 3C). When the cleavage sites were mapped and displayed onto the three-dimensional structure of the catalytic subunit, the majority of the cleavages occurred in the loop and turn regions (Figure 3D). This is consistent with the fact that loops and turns are usually more flexible and exposed to solvent and, thus, more accessible to cleavage by the free radicals. Some cleavage products were more predominant, indicating that these regions were "hot spots" for cleavage.

Conformational Switch from Open to Closed Conformation Induced by Binding of both MgATP and PKI. Binding of both MgATP and PKI to the C subunit leads to a switch from a more open to a closed conformation. To examine the conformational effects of ATP and PKI binding, we compared the footprinting patterns of free C and C·PKI·MgATP to identify locations in C that underwent significant changes in susceptibility to Fe−EDTA-mediated cleavage upon switching from the open to closed conformation (Figure 4). The majority of changes induced by binding of MgATP and PKI were localized at the N-terminal two-thirds of C (Figure 4A). Cleavage sites at 55, 70, 129, 140, 160, 167, 176, 188, 204, 219, and 230 (gray arrows) showed decreased susceptibility to Fe−EDTA mediated cleavage, while sites 61, 81, and 115 (black arrows) showed increased susceptibility to Fe−EDTA-mediated cleavage in the presence of MgATP. Cleavage site 49 (open arrow) "shifted" to a more C-terminal position (Figure 4A). This apparent "bandshift" is most likely due to a combination of a decrease in susceptibility to cleavage at site 49 and an increase in

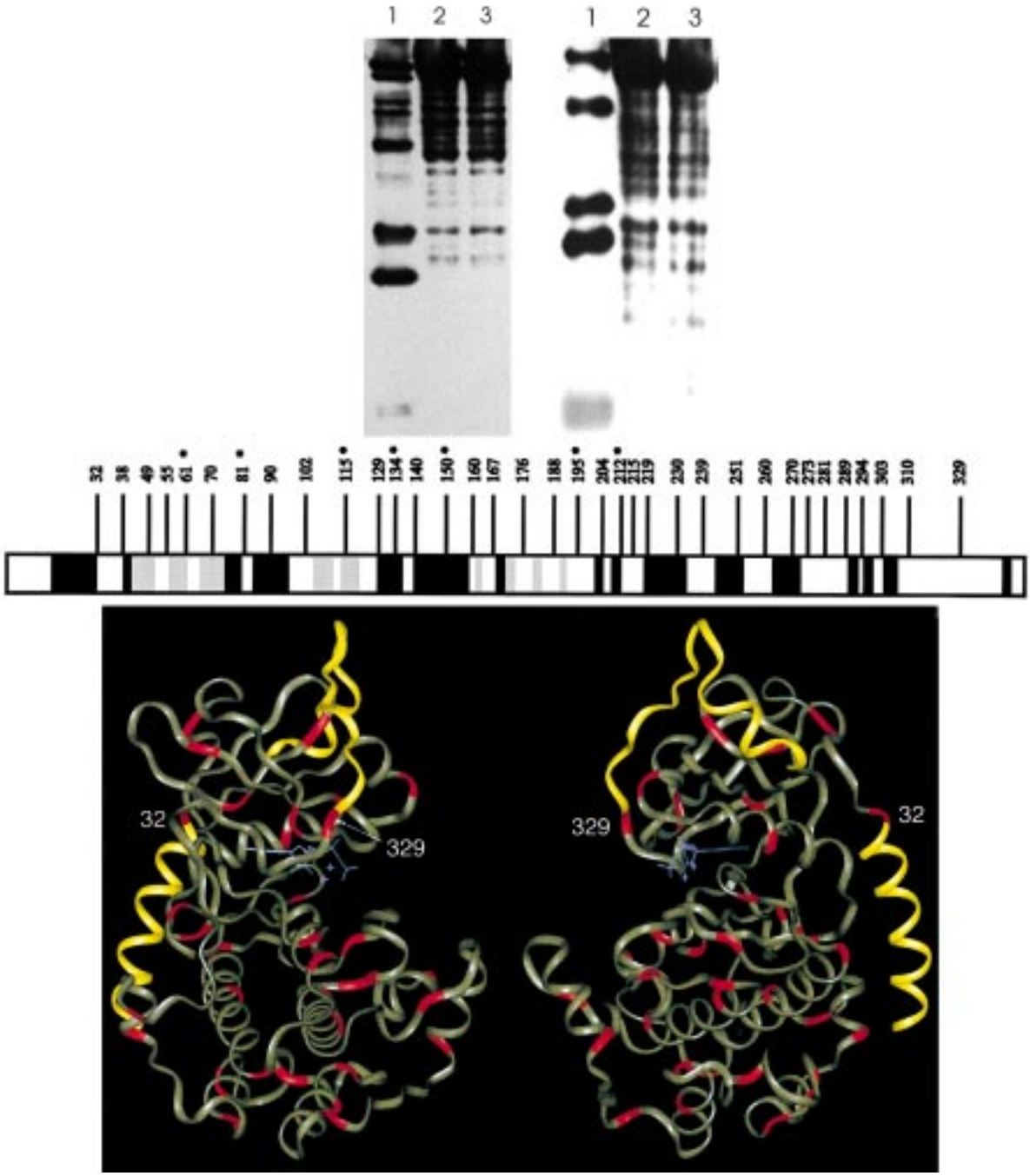

FIGURE 3: Identification of Fe−EDTA cleavage products of the catalytic subunit of cAPK. (A, top left) Fe−EDTA cleavage products probed by anti C-terminal antibodies. Lanes: 1, Met- and Trp-specific partially cleaved catalytic subunit molecular weight standards; 2 and 3, Fe−EDTA cleaved catalytic subunit. (B, top right) Fe−EDTA cleavage products detected by anti N-terminal antibodies. Lanes are the same as in (A). (C, middle) Summary of Fe−EDTA cleavage sites on the catalytic subunit of cAPK probed by anti N- and C-terminal antibodies. Each vertical line represents a cut along the amino acid sequence of the catalytic subunit with an asterisk indicating the most extensive cleavage sites. Black and gray bars represent α-helices and β-strands, respectively. (D, bottom) Schematic representation of Fe−EDTA cleavage sites in the three-dimensional structure of the catalytic subunit. The region of the catalytic subunit that is detectable by Fe−EDTA footprinting is colored in olive green, and specific cleavage sites are shown in red. The figure was drawn with Insight II (Molecular Simulations) using coordinates for C·ATP·PKI (*8*; Brookhaven Protein Data Bank accession 1atp).

susceptibility to cleavage at about position 51. These changes are localized primarily in four regions. (1) Residues 49−81 in the small lobe include the conserved glycine-rich loop, part of β-strand 1, and β-strands 2 and 3. This region is directly involved in the binding of the adenine ring and phosphates of ATP. (2) Residues 115−129 contain the linker strand that connects the small and large lobes. This region lines the packet where the nucleotide binds and also interacts directly with the adenine and ribose rings of ATP. (3) Residues 160−188 include the active center of the catalytic subunit that contains β-strands 6, 7, and 8 as well as the Mg positioning loop, the catalytic loop, and the activation loop. (4) Residues 219−230 include the F helix that stabilizes the catalytic loop (*5*, *7*−*9*). Most of the conserved residues that cluster around the active site reside within these regions. No significant changes were observed at the C-terminal one-third part of C (239−350) upon binding of MgATP and PKI (Figure 4B).

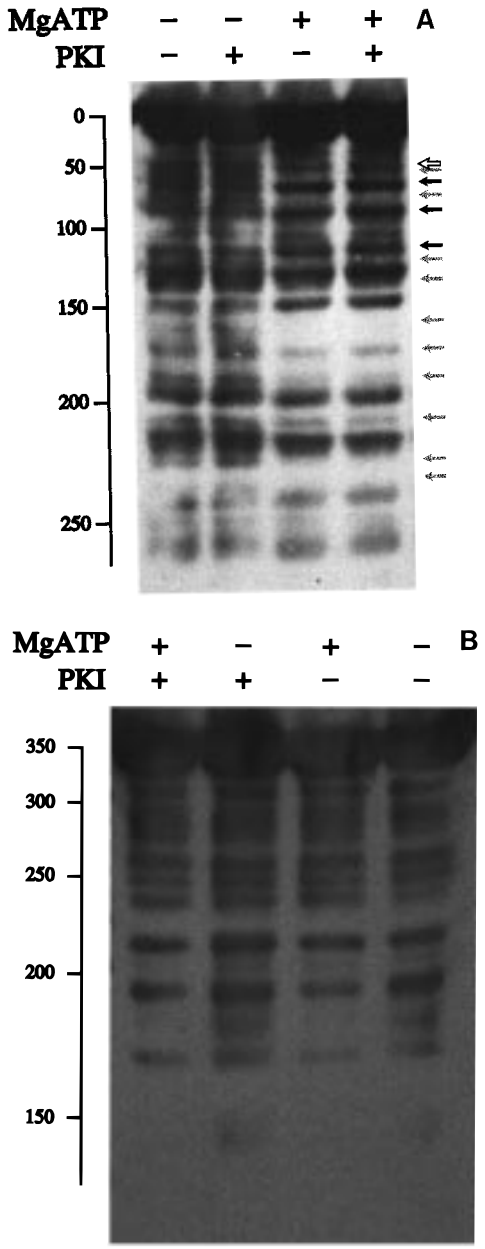

FIGURE 4: Protein footprinting analysis of the catalytic subunit of cAPK interactions with its substrate MgATP and inhibitor PKI. Fe−EDTA cleavage products of the catalytic subunit in the presence or absence of MgATP and PKI were detected by immunoblot stained with anti C-terminal C antibodies (A) or anti N-terminal C antibodies (B). The gray and black arrows show cleavage sites with decreased or increased susceptibility, respectively. The open arrow shows the cleavage site that shifts location from free C to the C·MgATP complex.

Conformational Changes Associated with Individual Binding of MgATP and PKI. Following analysis of the free C subunit and the ternary complex containing C, MgATP, and PKI, the effect of MgATP and PKI alone on cleavage was evaluated. As indicated in Figure 4, the addition of PKI alone had negligible effect. Cleavage of the C·PKI complex was indistinguishable from free C. In contrast to PKI, MgATP alone had a major effect on the susceptibility of the enzyme to cleavage. Furthermore, the pattern of cleavage products was indistinguishable from the pattern observed for the ternary complex. The results suggest that MgATP is having a major effect on the conformational state of the enzyme.

DISCUSSION

The crystal structures of the C-subunit reveal two distinctive conformational states: one in a more open and malleable conformation and the other in a closed conformation (*21*). On the basis of the orientation of the active site residues, it is evident that closing of the active site cleft must occur in order to position the terminal phosphate of ATP in close proximity to the peptide or protein substrate and is thus critical for the phophoryl transfer step (*39*). On the other hand, at least partial opening of the active site cleft is essential for binding and release of the nucleotide. Opening and closing is thus a prerequisite for normal catalysis (*18*, *19*). Whether the binding of either ATP or substrate peptide alone is capable of triggering a switch of equilibrium between open and closed conformations has been unclear. Using hydroxyl free radicals generated by reduction of an Fe−EDTA complex as a cleavage reagent, we mapped the solvent-accessible surface of the catalytic subunit of cAPK. Conformational changes in C induced by binding of substrates were probed by comparing specifically the footprinting patterns of free C, C·PKI, C·MgATP, and C·PKI·MgATP under conditions that reflect general physiological concentrations.

The cleavage patterns of free C and the ternary complex (C·PKI·MgATP) were distinct and confirmed that the enzyme undergoes global conformational changes as a consequence of both MgATP and PKI binding. The effects of each ligand alone showed striking differences. The cleavage patterns of free C and C·PKI were essentially identical, indicating that binding of PKI does not cause global changes in conformation. Although this observation is somewhat surprising because PKI makes extensive interactions with the catalytic subunit, it is consistent with crystallographic observations. Specifically, the crystal structure of a binary complex of the catalytic subunit and adenosine revealed no significant conformational changes in regions of the conserved large lobe where the inhibitor peptide docks compared to previously solved binary and ternary structures that all contained peptide (*40*). Furthermore, both open and closed conformations have been observed in binary complexes of C and PKI inhibitor peptides (*22*). Thus, on the basis of both footprinting and crystallographic results, the large lobe appears to serve as a stable docking surface for the peptide inhibitor. Binding of PKI does not induce either local or global changes in cleavage accessibility of a surface spanning from residues 32 to 329, and peptide backbones within the surface on which PKI docks are not sensitive to Fe−EDTA cleavage in either the presence or absence of PKI. An earlier study showed that cleavage of the malleable C-terminal tail outside the conserved kinase core between residues 332 and 333 by a kinase-splitting membranal proteinase was influenced by PKI (*41*). However, this cleavage site lies outside the range that can be probed by the footprinting technique described here. In addition, proteases, much larger than the free radicals used in chemical footprinting, are more prone to steric factors.

In contrast to PKI, the addition of MgATP alone had a significant effect on the conformation of the C subunit. These effects were both local due to direct interactions with the protein and global. Furthermore, protein footprinting of C·MgATP and C·PKI·MgATP gave nearly identical patterns,

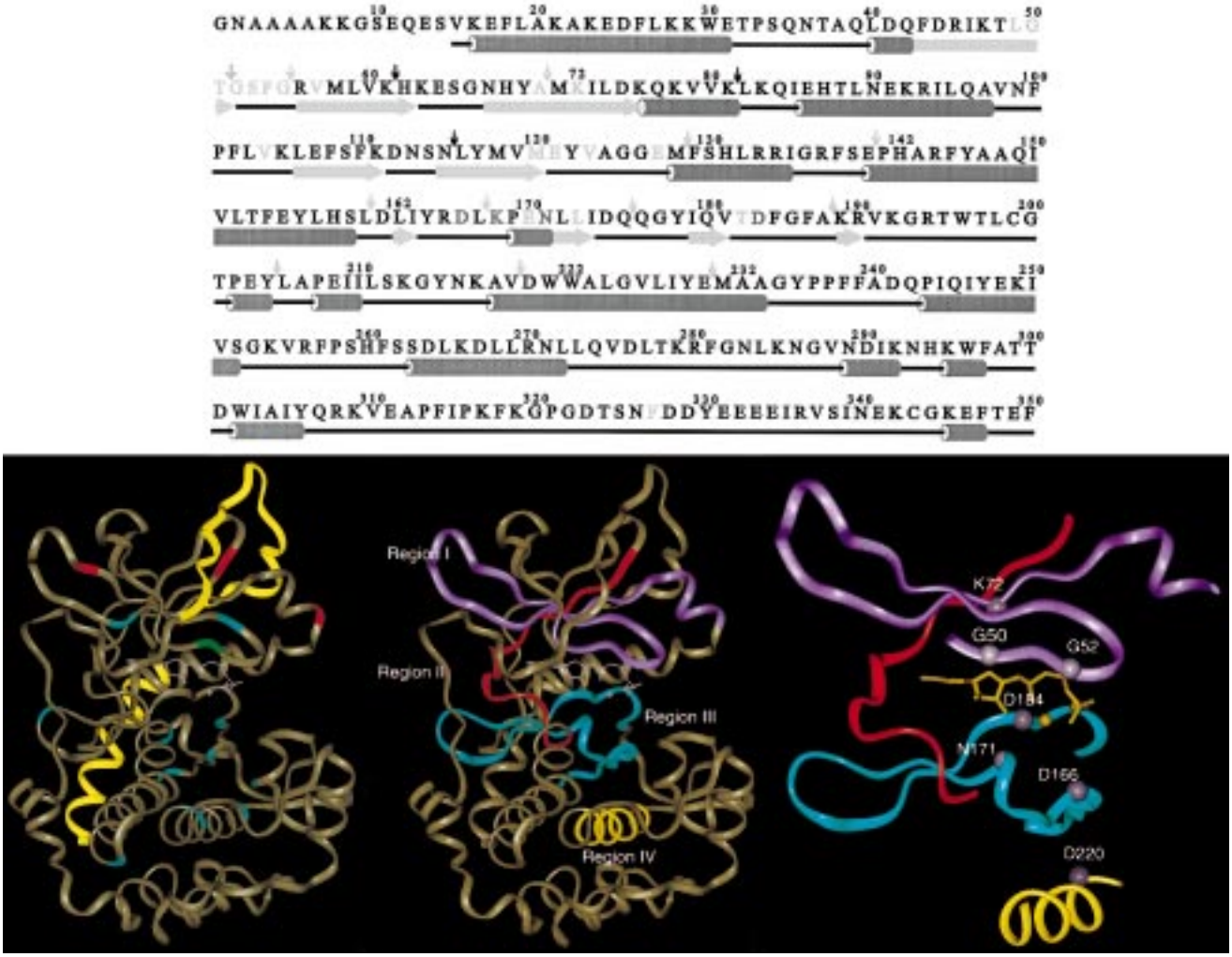

FIGURE 5: Localization of protein regions on the catalytic subunit affected by MgATP binding probed by Fe−EDTA protein footprinting. (A, top) Fe−EDTA cleavage sites affected by MgATP binding are shown along the polypeptide sequence of the catalytic subunit with gray arrows representing a decrease in cleavage and black arrows representing an increase in cleavage. The open arrow shows the cleavage site that shifts location from free C to the C·MgATP complex. Amino acid residues that interact with ATP and Mg^{2+} are shown in light and dark gray, respectively. (B, bottom left) Locations of cleavage sites affected by MgATP binding in the three-dimensional structure of the catalytic subunit are highlighted with different colors: cyan, decrease in susceptibility; red, increase in susceptibility; and green, shift of cleavage site. (C, bottom center) Structural representation of protein regions that are affected by MgATP binding in the three-dimensional structure of the catalytic subunit. The glycine-rich loop and β-strands 2 and 3 in the small lobe are shown in magenta (region I), the hinge that connects the small and large lobes is shown in red (region II), the Mg positioning loop, the catalytic loop, and part of the activation loop are shown in turquoise (region III), and the F helix is shown in yellow (region IV). (D, bottom right) Invariant residues that are important for all protein kinases within the four regions are highlighted in gray dots.

suggesting that the observed effects of MgATP and PKI on the chemical footprinting of C are due primarily to MgATP. This is consistent with the following previous results based on differential labeling. (1) MgATP alone afforded substantial protection of lysine residues by modification with acetic anhydride, and protection of some of these lysine residues were further enhanced by the addition of PKI(5−24) (*42*). (2) MgATP also protected against modification of carboxylates by a water-soluble carbodiimide (*43*). (3) MgATP protected against modification of the two cysteines, Cys199 and Cys343 (*44*). The effect of salts on the reactivity of the cysteines was the first evidence to suggest that the C subunit was a very malleable protein (*45*, *46*).

Several regions (49−81, 115−129, 160−188, and 219−230) showed significant structural perturbation upon MgATP binding (Figures 4 and 5). These regions correlate well with the structural data and are indicative of global conformational changes in the protein. In the C·MgATP·IP20 ternary complex, MgATP is deeply buried, sandwiched between the small and large lobes. The adenine ring is enclosed in a hydrophobic pocket formed at the domain interface and consists of residues from the small lobe (Leu49, Val57, Ala70), the large lobe (Leu173), and a small linker segment (Met120 through Val123) that connects the two lobes (*8*). The phosphates of ATP also interact with both the small and large lobes. Lys72 in β-strand 3 interacts with the α- and β-phosphates. The β-phosphate in addition is held by interactions with the backbone amides of Phe54 and Gly55 from the glycine-rich loop between β-strands 1 and 2 while the Ser53 amide at the tip of the loop hydrogen bonds to the γ-phosphate of ATP (*47*). Residues 166−171 from the catalytic loop in the large lobe with Lys168 interact specifically with the γ-phosphate to facilitate catalysis. The Mg ions are coordinated by oxygens of the β- and γ-phosphates of ATP, by three solvent molecules, and by the invariant Asp184 from the adjacent Mg positioning loop between

β-strands 8 and 9. The second Mg ion bridging the α- and γ-phosphates is coordinated by Asn171 and Asp184. The 2′- and 3′-OH groups from the ribose ring are held by interactions with side chains 127 and Glu170, respectively (*8*). Our footprinting results identified all the sites that are in direct contact with MgATP in the closed conformation. In addition, perturbations around the activation loop and the F helix were also identified. Neither of these structural elements interacts directly with MgATP, although the reactivity of Cys199 in the activation loop is reduced dramatically by MgATP binding (*44*), and the F helix contains one highly conserved residue, Asp220, which helps to stabilize the catalytic loop (*8*). These long-range effects support the idea of an extensive network that is important for the global conformational switches that are critical for the dynamic catalytic process.

The decreased susceptibility to cleavage observed upon MgATP binding may be due to induced global conformational changes, to the protection of residues that come in direct contact with the ligand, or to a combination of both. We cannot distinguish these two possibilities using the protein footprinting technique; however, correlation of the changes in cleavage with the structure confirms that the effects are both local and global. That is the advantage of this nonspecific method of mapping with a small reagent. It identifies both local and global changes while other methods such as affinity labeling identify only specific residues that contribute directly to ligand binding. In addition, the area that a small molecule, MgATP, can shield does not match the large and extensive changes observed by the protein footprinting in this study. Therefore, conformational changes must occur upon MgATP binding so that the closed conformation observed in the crystal structure of the ternary complex of C is already mostly favored in solution when MgATP binds. PKI directly shields a larger surface but does not lead to global changes.

The structural elements affected by MgATP binding are highlighted in Figure 5. The glycine-rich loop and β-strands 1 and 2 in the small lobe, the catalytic loop, the Mg positioning loop, and part of the activation loop from the large lobe form the linings of the domain interface which in turn is connected by the linker strand. These structural components together form a "clamp" to firmly hold the MgATP inside the active cleft (Figure 5C,D). These extensive structural perturbations induced by MgATP are consistent with a transition from a looser open conformation to the closed conformation which is essential for phosphoryl transfer. The binding of MgATP thus appears to be "priming" the enzyme for catalysis. Since many of the highly conserved residues in the catalytic core lie in the regions that are affected by binding of MgATP (Figure 5D), these conformational changes induced upon MgATP binding may also apply more generally to other protein kinases in the family.

Kinetic studies suggest that there is a preferred order of binding substrates, with the nucleotide binding first followed by peptide (*48*, *49*). High-affinity binding of PKI requires the synergistic binding of MgATP; PKI binds C with apparent K_d's of 0.2 nM and 2.3 μM in the presence and absence of MgATP, respectively (*50*), representing a 5-order magnitude difference. Protein footprinting suggests that MgATP increases PKI affinity by shifting the equilibrium to the closed conformation which is then primed for the high-affinity docking of PKI.

In summary, we demonstrate that the protein footprinting approach is a very sensitive technique for monitoring conformational changes in proteins with relatively high resolution. The technique is complementary to crystallographic studies because it probes structural changes under equilibrium solution conditions. Consequently, many conditions can be examined in parallel to provide valuable information on changes in conformation or dynamics. Some of the most intensive cleavage sites of the C-subunit by Fe−EDTA occur around regions 61, 81, 115, 134, 150, 195, and 215 (Figure 3C). These hot spots correlate very well with some of the most flexible regions in the C-subunit identified by molecular dynamics calculations (Tsigelny and Ten Eyck, personal communication). Thus protein footprinting is potentially useful for mapping protein dynamics and regions of high flexibility. Using Fe−EDTA-mediated protein footprinting, we accurately identified the conformational changes in the catalytic subunit upon binding of substrates. Most important, our results indicate that binding of MgATP is one of the most crucial steps in the catalytic mechanism of cAPK. Binding of MgATP induces extensive conformational changes in the catalytic subunit of cAPK that lead to the closure of the active site and primes the catalytic subunit poised in a conformation that is favorable for catalysis in response to subsequent binding of peptide substrates.

REFERENCES

1. Hanks, S. K., Quinn, A. M., and Hunter, T. (1988) *Science 241*, 42−52.
2. Taylor, S. S., Buechler, J. A., and Knighton, D. (1990) in *Peptides and Protein Phosphorylation* (Kemp, B. E., Ed.) pp 1−41, CRC Press, Boca Raton, FL.
3. Beebe, S. J., and Corbin, J. D. (1986) in *The Enzymes: Control by Phosphorylation, Part A* (Krebs, E. G., and Boyer, P. D., Eds.) Vol. XVII, pp 43−111, Academic Press, Inc., New York.
4. Taylor, S. S., Buechler, J. A., and Yonemoto, W. (1990) *Annu. Rev. Biochem. 59*, 971−1005.
5. Knighton, D. R., Zheng, J., Ten Eyck, L. F., Ashford, V. A., Xuong, N.-h., Taylor, S. S., and Sowadski, J. M. (1991) *Science 253*, 407−414.
6. Taylor, S. S., Knighton, D. R., Zheng, J., Ten Eyck, L. F., and Sowadski, J. M. (1992) *Annu. Rev. Cell Biol. 8*, 429−462.
7. Taylor, S. S., and Radzio-Andzelm, E. (1994) *Structure 2*, 345−355.
8. Zheng, J., Knighton, D. R., Ten Eyck, L. F., Karlsson, R., Xuong, N.-h., Taylor, S. S., and Sowadski, J. M. (1993) *Biochemistry 32*, 2154−2161.
9. Knighton, D. R., Zheng, J., Ten Eyck, L. F., Xuong, N.-h., Taylor, S. S., and Sowadski, J. M. (1991) *Science 253*, 414−420.
10. De Bondt, H. L., Rosenblatt, J., Jancarik, J., Jones, H. D., Morgan, D. O., and Kim, S. H. (1993) *Nature 363*, 595−602.
11. Jeffrey, P. D., Russo, A. A., Polyak, K., Gibbs, E., Hurwitz, J., Massague, J., and Pavletich, N. P. (1995) *Nature 376*, 313−320.
12. Zhang, F., Strand, A., Robbins, D., Cobb, M. H., and Goldsmith, E. J. (1994) *Nature 367*, 704−711.
13. Wilson, K. P., Fitzgibbon, M. J., Caron, P. R., Griffith, J. P., Chen, W., McCaffrey, P. G., Chambers, S. P., and Su, M. S.-S. (1996) *J. Biol. Chem. 271*, 27696−27700.
14. Wang, Z., Harkins, P., Ulevitch, R., Han, J., Cobb, M. H., and Goldsmith, E. J. (1997) *Proc. Natl. Acad. Sci. U.S.A. 94*, 2327−2332.
15. Xu, W., Harrison, S. C., and Eck, M. J. (1997) *Nature 385*, 595−602.

16. Canagarajah, B. J., Khokhlatchev, A., Cobb, M. H., and Goldsmith, E. J. (1997) *Cell 90*, 859−869.
17. Shoji, S., Titani, K., Demaille, J. G., and Fisher, E. G. (1979) *J. Biol. Chem. 254*, 6211−6214.
18. Grant, B. D., and Adams J. A. (1996) *Biochemistry 35*, 2022−2029.
19. Lew, J., Coruh, N., Tsigelny, I., Garrod, S., and Taylor, S. S. (1996) *J. Biol. Chem. 272*, 1507−1513.
20. Knighton, D. R., Bell, S. M., Zheng, J., Ten Eyck, L. F., Xuong, N.-h., Taylor, S. S., and Sowadski, J. M. (1993) *Acta Crystallogr. D49*, 357−361.
21. Zheng, J., Knighton, D. R., Xuong, N.-h., Taylor, S. S., Sowadski, J. M., and Ten Eyck, L. F. (1993) *Protein Sci. 2*, 1559−1573.
22. Karlsson, R., Zheng, J., Xuong, N.-h., Taylor, S. S., and Sowadski, J. M. (1993) *Acta Crystallogr. D49*, 381−388.
23. Bossemeyer, D., Engh, R. A., Kinzel, V., Ponstingl, H., and Huber, R. (1993) *EMBO J. 12*, 849−859.
24. Heyduk, E., and Heyduk, T. (1994) *Biochemistry 33*, 9643−9650.
25. Hanai, R., and Wang, J. C. (1994) *Proc. Natl. Acad. Sci. U.S.A. 91*, 11904−11908.
26. Zhong, M., Lin, L., and Kallenbach, N. R. (1995) *Proc. Natl. Acad. Sci. U.S.A. 92*, 2111−2115.
27. Jensen, T. H., Leffers, H., and Kjems, J. (1995) *J. Biol. Chem. 270*, 13777−13784.
28. Hori, R., Pyo, S., and Carey, M. (1995) *Proc. Natl. Acad. Sci. U.S.A. 92*, 6094−6051.
29. Greiner, D. P., Hughes, K. A., Gunasekera, A. H., and Meares, C. F. (1996) *Proc. Natl. Acad. Sci. U.S.A. 93*, 71−75.
30. Heyduk, T., Heyduk, E., Severinov, K., Tang, H., and Ebright, R. H. (1996) *Proc. Natl. Acad. Sci. U.S.A. 93*, 10162−10166.
31. Baichoo, N., and Heyduk, T. (1997) *Bicohemistry 36*, 10830−10836.
32. Slice, L. W., and Taylor, S. S. (1989) *J. Biol. Chem. 264*, 20940−20946.
33. Herberg, F. W., Bell, S. M., and Taylor, S. S. (1993) *Protein Eng. 6*, 771−777.
34. Richardson, J. M., Howard, P., Massa, J. S., and Maurer, R. A. (1990) *J. Biol. Chem. 265*, 13635−13640.
35. Chestukhin, A., Litovchick, L., Batkin, M., and Shaltiel, S. (1996) *FEBS Lett. 383*, 265−270.
36. Schägger, H., and Von Jagow, G. (1987) *Anal. Biochem. 166*, 138−379.
37. Jue, R. A., and Doolittle, R. F. (1985) *Biochemistry 24*, 162−170.
38. Brenowitz, M., Senear, D., Shea, M. A., and Ackers, G. K. (1986) *Methods Enzymol. 30*, 133−181.
39. Grant, B. D., Hemmer, W., Tsigelny, I., Adams, J. A., and Taylor, S. S. (1998) *Biochemistry 37*, 7708−7715.
40. Narayana, N., Cox, S., Xuong, N.-h., Ten Eyck, L. F., and Taylor, S. S. (1997) *Structure 5*, 921−935.
41. Chestukhin, A., Litovochick, L., Schourov, D., Cox, S., Taylor, S. S., and Shaltiel, S. (1996) *J. Biol. Chem. 271*, 10175−10182.
42. Buechler, J. A., Vedvick, T. A., and Taylor, S. S. (1989) *Biochemistry 28*, 3018−3024.
43. Buechler, J. A., and Taylor, S. S. (1990) *Biochemistry 29*, 1937−1943.
44. Nelson, N. C., and Taylor, S. S. (1981) *J. Biol. Chem. 256*, 3743−3750.
45. Jiménez, J. S., Kupfer, A., Gani, V., and Shaltiel, S. (1982) *Biochemistry 21*, 1623−1630.
46. Shaltiel, S., Cox, S., and Taylor, S. S. (1998) *Proc. Natl. Acad. Sci. U.S.A. 95*, 484−491.
47. Bossemeyer, D. (1994) *Trends Biochem. Sci. 19*, 201−205.
48. Whitehouse, S., and Walsh, D. A. (1983) *J. Biol. Chem. 258*, 3682−3692.
49. Whitehouse, S., Feramisco, J. R., Casnellie, J. E., Krebs, E. G., and Walsh, D. A. (1983) *J. Biol. Chem. 258*, 3693−3701.
50. Herberg, F. W., and Taylor, S. S. (1993) *Biochemistry 32*, 14025−14022.

BI981057P